

A novel dual independent control for a quasi Z source inverter driven electromagnetic actuator based energy harvesting system

M. A. Hasan, Naresh. K. Vemula, Ramesh Devarapalli, and Łukasz Knypinski

Abstract—This paper proposes a Z source inverter assisted electromagnetic energy harvesting system. Electrical and mechanical components in an energy harvesting system produces electrical energy when tuned optimally. Adjustment of damping and resonant frequency is a crucial parameter in operating an energy harvesting system. This paper proposes a Z source inverter assisted system, where the independent control freedom of Z source inverter has been utilized to regulate the output power. The two key components, damping and resonant frequency, have been regulated and therefore, an improved performance of the energy harvesting system has been achieved. The simulation based validation establishes the effectiveness of proposed architecture and control under operating conditions of varying frequency and varying amplitude.

Keywords—Electromagnetic Actuator; Z-Source Inverter; Damping; Resonant frequency; Active Power Control; Reactive Power Control

I. INTRODUCTION

ELECTROMAGNETIC actuator-based energy harvester systems have been a subject of significant research interest due to their potential to convert ambient mechanical energy into usable electrical energy for powering small-scale electronic devices. These systems typically operate on the principle of electromagnetic induction, where a motion-induced change in magnetic flux generates an electromotive force (EMF) across a coil, thereby producing electric current [1], [2]. One of the key challenges in designing efficient electromagnetic energy harvesters is to ensure that the harvester's resonant frequency matches the frequency of the ambient vibrations [3]–[5]. This is crucial for maximizing the power output, as the harvester's performance is optimal when it operates in resonance with the excitation source [6]. Several methods have been proposed to achieve this frequency matching, including mechanical tuning techniques that modify the spring constant

M. A. Hasan is with Electrical and Electronics Engineering Department, Birla Institute of Technology, Ranchi, India (e-mail: asifhasan@bitmesra.ac.in).

Naresh K. Vemula is with the Department of Electrical and Electronics Engineering, SRM University AP, Amaravati, India (e-mail: nareshkumar12523@gmail.com).

Ramesh Devarapalli is with the Department of Electrical/Electronics and Instrumentation Engineering, Institute of Chemical Technology, Indian Oil Odisha Campus, Bhubaneswar (e-mail: dr.r.devarapalli@gmail.com).

Łukasz Knypinski is with the Faculty of Automatic Control, Robotics and Electrical Engineering, Poznan University of Technology, Poznan, Poland (e-mail: lukasz.knypinski@put.poznan.pl).

or mass of the system, and electrical tuning methods that adjust the electrical load seen by the transducer [7]–[13].

Mechanical tuning methods, such as those employing electrostatic actuators or magnetic tuning mechanisms, can effectively adjust the resonant frequency [14]. However, these methods often increase system complexity and require additional actuation mechanisms, which may consume a portion of the harvested energy and add to the overall volume and cost of the system [15]. In contrast, electrical tuning methods offer a more versatile and potentially less energy-intensive approach to adjusting the resonant frequency. One such method involves the use of discrete reactive components (inductors and capacitors) to modify the electrical load [16]. While this approach can shift the resonant frequency, it is limited to a finite set of discrete frequencies and does not allow for continuous tuning.

A notable advancement in the field of electromagnetic energy harvesting is the development of power electronic interfaces capable of continuously tuning the resonant frequency and damping of the harvester. Literature review presents a novel technique using an H-bridge power electronic interface to synthesize a range of complex load impedance values, enabling continuous adjustment of the harvester's resonant frequency and damping [11]. This method overcomes the limitations of previous approaches by providing precise control over the tuning parameters and integrating rectification within the tuning interface, which allows for efficient energy storage into a battery. The H-bridge interface, as demonstrated in this paper can mimic the electrical characteristics of inductors, capacitors, or resistors by controlling the flow of real and reactive power between the mechanical system and the electrical load. This results in a system that can operate over an increased frequency range and can increase real output power by up to 25 percent. The technique also offers the advantage of being able to adjust the electrical damping to match the parasitic mechanical damping, further enhancing the power output of the harvester.

The H-bridge inverter topology, while popular for its simplicity and efficiency in converting DC to AC power, has several limitations that can impact its applicability in energy harvesting systems. One of the primary drawbacks is its lack of inherent voltage boost capability because of which, it cannot increase the input voltage from the energy source [17]. This can be a significant limitation when the harvested voltage is



low or fluctuates, requiring the addition of a separate boost converter, which adds complexity and cost to the system. Additionally, the H-bridge inverter has a limited input voltage range, which can be problematic in applications where the input voltage varies widely [18], [19]. Furthermore, it may not be as effective in handling low voltage levels without additional circuitry, reducing its efficiency in systems that produce variable or low power [20]–[22]. These limitations make the H-bridge inverter less suitable for applications requiring flexibility in input voltage handling or where maximizing power extraction from a variable source is critical.

Compared to H bridge inverter, the Z-source inverter topology offers significant advantages in energy harvesting systems, particularly due to its unique ability to both boost and buck the input voltage. Unlike traditional inverter topologies, the Z-source inverter employs a special impedance network composed of inductors and capacitors, which allows it to increase the input voltage without the need for a separate boost converter. This capability is especially beneficial in energy harvesting applications where the harvested voltage may be low or variable, ensuring that the system can still produce a usable output even when the input voltage fluctuates. This single-stage voltage conversion simplifies the overall system design, reducing the need for additional components and enhancing efficiency. Another major advantage of the Z-source inverter is its wide input voltage range, making it highly adaptable to various energy harvesting scenarios. In systems where the input voltage is not consistent—such as those powered by intermittent or irregular energy sources like human motion or environmental vibrations—the Z-source inverter can maintain efficient operation across a broad spectrum of input conditions. This flexibility makes it an excellent choice for maximizing power extraction in situations where other inverter topologies might struggle to perform effectively. Additionally, the Z-source inverter enhances system reliability by offering protection against electrical faults, such as shoot-through, which can occur in traditional inverter designs. The impedance network provides a built-in defense against such faults, reducing the risk of damage and improving the overall durability of the energy harvesting system. This added reliability, coupled with the inverter's flexibility and efficiency, makes the Z-source inverter particularly well-suited for energy harvesting applications that require robust and consistent performance despite varying input conditions.

Because of superior performance of Z source inverter topology over H bridge, this paper proposes a novel Z source impedance based scheme for actuator based energy harvesting system. An architecture to harness the motion based energy through actuator with the help of an interfacing Z source inverter has been presented. The detailed mathematical modeling of the proposed system has been developed. A suitable control strategy for maintaining the desired damping and resonance frequency through Z source inverter has been developed and presented. The simulation based validation presents the effectiveness of the proposed system with increased efficiency and superior performance.

II. THE PROPOSED ENERGY HARVESTING SYSTEM WITH Z SOURCE INVERTER

The proposed actuator-based energy harvesting system is designed to convert mechanical energy, such as vibrations or human motion, into electrical energy using an electromagnetic actuator. This actuator consists of a magnet, coil, spring, and damping mechanism. As the magnet oscillates due to mechanical motion, it induces an electromotive force (EMF) in the coil, converting kinetic energy into electrical energy. The system employs a Z-source impedance inverter to manage and optimize the harvested energy. Unlike traditional inverters, the Z-source inverter features an impedance network composed of inductors and capacitors. With the help of a diode in the circuit, this network allows the inverter to perform both voltage boost and regulation without the need for an additional DC-DC converter, making it highly efficient and adaptable to varying input voltages. Figure 1 presents the overall architecture of the proposed energy harvesting system. The actuator-based energy

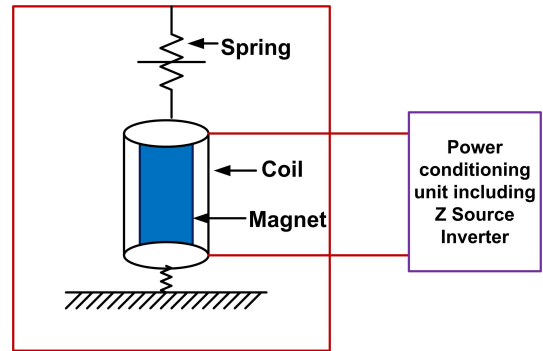


Fig. 1. Proposed architecture of the actuator based energy harvesting system

harvesting system is represented by an electrical equivalent circuit that models the conversion of mechanical energy into electrical energy. Figure 2 presents the electrical equivalent circuit of the overall energy harvesting system. This circuit includes a dependent current source, which is influenced by factors such as the actuator's excitation frequency, the amplitude of the mechanical input, and the mass exerting force on the actuator. The dependent current source symbolizes the mechanical energy being converted into electrical energy by the actuator. Connected in parallel to this current source is an RLC circuit, which represents the mechanical properties of the actuator. In this circuit, the resistance accounts for parasitic damping, the inductance corresponds to the mass of the system, and the capacitance reflects the spring constant. These elements capture the dynamic response of the actuator to mechanical excitation, illustrating how energy is stored and dissipated. The electromagnetic transduction mechanism, which is responsible for converting mechanical energy into electrical energy, is modeled by a transformer in the circuit. The mechanical side of the actuator is connected to the primary side of the transformer, while the secondary side is linked to parasitic inductance and resistance. These parasitic components represent the losses and inefficiencies in the system that do not contribute to useful electrical output.

Finally, the circuit includes a load that is connected to the secondary side of the transformer through a single-phase Z-source inverter. The Z-source inverter plays a crucial role in processing the harvested energy, converting the DC voltage from the actuator into a stable AC output suitable for powering the load. This inverter is particularly effective in handling variations in input voltage, ensuring that the system operates efficiently across a wide range of conditions. The described

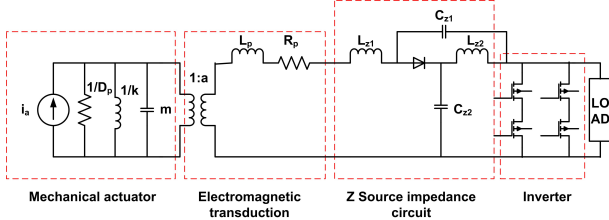


Fig. 2. Electrical equivalent circuit of the actuator based energy harvesting system

Z-source impedance inverter circuit features a unique configuration designed to efficiently convert and regulate electrical energy. The circuit begins with an inductor connected in series with a forward-biased diode, followed by another inductor. This sequence of components is crucial for energy storage and current regulation within the circuit. The first inductor, located at the beginning of the series, stores energy in its magnetic field when current flows through it. This inductor is followed by a forward-biased diode, which allows current to pass through in the forward direction while blocking any reverse current, ensuring unidirectional flow. After the diode, the second inductor continues to store energy, further smoothing the current and providing a stable flow through the circuit.

In addition to these series components, the circuit includes two capacitors strategically placed to form an impedance network. The first capacitor is connected between the P terminal of the diode and the positive bus of the inverter. This capacitor stores energy in its electric field, providing a buffer that helps maintain a steady voltage across the inverter's positive bus. The second capacitor is connected between the N terminal of the diode and the inverter's negative bus. This capacitor similarly stabilizes the voltage on the negative side of the inverter, ensuring a balanced operation of the circuit. Together, these inductors and capacitors form an impedance network that enables the Z-source inverter to perform both voltage boost and buck operations. The capacitors work in conjunction with the inductors to regulate the voltage across the inverter, allowing it to adapt to varying input conditions and maintain a consistent output. The forward diode plays a critical role in directing the flow of current, ensuring that the energy stored in the inductors is properly utilized during the operation of the inverter. This configuration enhances the inverter's flexibility and efficiency, making it particularly suitable for applications where input voltages are variable or need to be adjusted to match load requirements.

A. Mathematical Modeling of the Proposed Energy Harvesting System

A detailed mathematical model for the proposed electromagnetic actuator-based energy harvester system has been developed in this section. It involves analyzing the dynamics of the system, the electromagnetic induction process, and the power generation. The external force applied on the magnet, because of human motion, has been considered as a periodic movement and represented as,

$$F(t) = F_0 \sin(\omega t) \quad (1)$$

where F_0 is the magnitude of applied external force and the ω is the angular frequency of the applied force. The dynamics of the magnetic movement is governed by the below given equation,

$$m \frac{d^2 x(t)}{dt^2} + c \frac{dx(t)}{dt} + kx(t) = F(t) \quad (2)$$

where, M is the mass of the magnet, C is damping coefficient, K is spring constant and $x(t)$ is the displacement of the magnet. With the mentioned displacement, an emf will be induced in the coil surrounding the magnet given as follows,

$$e(t) = N B A k_m \sin(k_m x(t)) \frac{dx(t)}{dt} \quad (3)$$

where, N is the number of turns in the surrounding coil, B is the magnetic field strength, A is the effective area of the coil and k_m is the proportionality constant. For small displacements, the induced emf expression can be simplified as follows,

$$e(t) = N B A k_m \frac{dx(t)}{dt} \quad (4)$$

With the above dynamics, the natural frequency of the mechanical system will be,

$$\omega_n = \sqrt{\frac{k}{m}} \quad (5)$$

This is the frequency at which the system will naturally oscillate when it is disturbed. To analyze the response of the system, we solve the differential equation using the method of undetermined coefficients. For a sinusoidal force $F(t)$, the steady-state solution for $x(t)$ is obtained as follows,

$$x(t) = X \sin(\omega t - \phi) \quad (6)$$

where, X is the amplitude of steady state oscillation and ϕ is the phase difference of force and displacement. Solving above expression, we get,

$$X = \frac{X_0/m}{\sqrt{(\omega_n^2 - \omega^2)^2 + (\frac{c\omega}{m})^2}} \quad (7)$$

The amplitude X reaches its maximum value when the denominator is minimized. This occurs when the excitation frequency ω equals the natural frequency ω_n . At resonance, the equation for X produces result as,

$$X = \frac{F_0}{c\omega_n} \quad (8)$$

As presented in equation (4), the induced emf is proportional to the velocity of the magnet. Since $x(t)$ is sinusoidal at resonance, the velocity $\frac{dx(t)}{dt}$ will also be sinusoidal with maximum amplitude at resonance. Therefore, the induced EMF $e(t)$ is maximized when the system is at resonance. The electrical power generated $P(t)$ is proportional to the square of the EMF. Thus, the power generated is maximized when the system operates at its resonant frequency, where the amplitude of oscillation X is maximum.

III. DUAL INDEPENDENT CONTROL OF Z SOURCE INVERTER

The quasi-Z-source inverter (qZSI) is a variant of the traditional Z-source inverter and it offers advantages such as reduced component stress, continuous input current, and easier control. The operation of the qZSI involves two distinct states: the shoot-through state and the non-shoot-through state. These states are fundamental to how the qZSI regulates voltage and provides the desired output. These states are demonstrated in Figure 3. In the non-shoot-through state, the qZSI operates

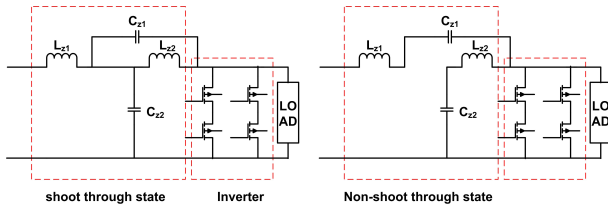


Fig. 3. Shoot through and non-shoot through state of Z source inverter circuit

similarly to a conventional inverter. In this state, none of the inverter switches are shorted simultaneously, and the inverter operates normally by transferring power from the DC source to the load. The DC input voltage is applied to the impedance network, consisting of inductors and capacitors. The energy stored in the inductors is transferred to the capacitors, and the power is delivered to the load through the inverter bridge. During this state, the diodes in the impedance network are reverse-biased, preventing any current from flowing back through them. The output voltage of the inverter is determined by the difference between the capacitor voltages and the voltage drop across the inductors.

In the shoot-through state, the qZSI allows the impedance circuit to short-circuit through any phase leg(s) of the inverter bridge without damaging the circuit. This state is crucial for boosting the DC voltage to a higher level before it is converted to AC. In this state, one or more switches in the same phase leg are turned on simultaneously, creating a short circuit across the inverter's output. During the shoot-through state, the inverter bridge is short-circuited, and the inductors store energy by drawing current from the DC source and the capacitors. The diodes in the circuit become forward-biased, allowing the inductors to charge and increase their energy. This process effectively boosts the voltage across the capacitors, enabling a higher voltage to be applied to the inverter when it returns to the non-shoot-through state.

The qZSI alternates between the shoot-through and non-shoot-through states, using the shoot-through state to boost

the voltage and the non-shoot-through state to deliver power to the load. The duration of the shoot-through state, controlled by the duty cycle D_s determines the amount of voltage boost.

A. Proposed Dual Control of Inverter

The boosting capacity of the inverter depends upon the shoot through and non-shoot through states duration and is given as follows,

$$B = \frac{1}{1 - 2D_s} \quad (9)$$

The output voltage, as regulated by inverter control, available at the load end is given as follows,

$$V_{out} = B * V_{in} * M \quad (10)$$

where, V_{in} is the voltage available before the quasi Z source circuit, V_{out} is the load voltage and M is the modulation index for the switching signal generation. A feedback control loop has been designed to implement the dual control of the inverter so as to achieve the maximum power output at resonant frequency from the energy harvesting system. The overall feedback control system is presented in Figure 4. The control of the quasi-Z-source inverter (qZSI) with

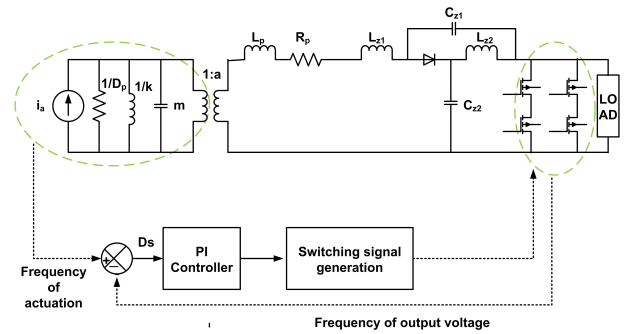


Fig. 4. Proposed dual close loop control structure for the energy harvesting system

adaptive resonance frequency control operates by dynamically adjusting key parameters to ensure that the electrical resonance frequency of the inverter matches the mechanical resonance frequency of the energy harvesting system. This dynamic matching is crucial for maximizing power transfer and efficiency in the system. The control system begins by continuously monitoring the mechanical resonance frequency of the actuator-based energy harvesting system using sensors. This mechanical resonance frequency can vary over time due to changes in the operating conditions, such as varying loads or environmental factors. Once the mechanical resonance frequency is determined, the control system calculates the required electrical resonance frequency that should be maintained by the qZSI. The electrical resonance frequency is a function of the effective inductance and capacitance in the impedance network of the qZSI. To match this calculated frequency with the varying mechanical resonance frequency, the control system adjusts the shoot-through duty cycle D_s of the inverter. The shoot-through duty cycle is a critical parameter that influences the energy stored in the inductors,

thereby affecting the effective inductance and capacitance of the impedance network. By increasing or decreasing D_s the control system can fine-tune the electrical resonance frequency to match the mechanical resonance frequency.

Simultaneously, the modulation index M , which controls the amplitude of the output voltage, is also adjusted in response to the desired output and the changes in D_s . The modulation index is responsible for determining the shape and magnitude of the inverter's output voltage waveform. The integration of shoot-through pulses into the PWM signals ensures that the inverter operates efficiently, with the shoot-through states providing the necessary voltage boost. The entire process is managed through a closed-loop control system that continuously monitors the output voltage, current, and mechanical resonance frequency. Feedback from these parameters allows the control system to make real-time adjustments to both D_s and M , ensuring that the system operates at the optimal point for maximum power density. This adaptive approach ensures that the electrical resonance frequency is always in sync with the mechanical resonance frequency, thereby optimizing the energy harvesting process and enhancing the overall performance and efficiency of the system.

IV. SIMULATION BASED VALIDATION OF PROPOSED SCHEME

The proposed architecture of actuator based energy harvesting system has been implemented in MATLAB/Simulink environment and the control has been applied to assess the performance of energy harvesting system under different operating conditions. In this study, extensive simulations were conducted to evaluate the performance of an actuator-based energy harvesting system under various operating conditions, focusing on the dynamics of the mechanical system. The key parameters investigated included changes in the amplitude of the force applied to the actuator and variations in the frequency of actuation. These factors are critical in understanding how the system responds to real-world conditions, where the force exerted on the actuator can fluctuate, and the actuation frequency may not remain constant.

The simulation framework has been so designed to mimic realistic scenarios where the mechanical system's dynamics are subject to change. For instance, the amplitude of the applied force was varied to assess how the energy harvesting efficiency and output power density were affected. This aspect of the study is crucial as it directly relates to the system's ability to harness energy from varying mechanical inputs, such as those encountered in environments with inconsistent or sporadic forces. Moreover, the frequency of actuation was systematically altered to explore the system's performance across a range of excitation frequencies. This analysis is particularly important for understanding the resonance characteristics of the system and how closely the electrical resonance frequency can be tuned to match the mechanical resonance frequency under different operating conditions. The ability to adapt to changing frequencies is vital for maximizing power transfer and ensuring the energy harvesting system operates at peak efficiency.

In the simulation study, both amplitude and frequency change scenarios have been analyzed to compare the performance of the actuator-based energy harvesting system when interfaced with a conventional H-bridge inverter and a Quasi Z-source inverter. parameters of the actuation system and power electronic interface are provided in Table 1.

TABLE I
SPECIFICATION OF ENERGY HARVESTING SYSTEM

S.No	Parameter	Symbol	Value
1	Mass of magnet	m	$1.77 * 10^{-3}$ Kg
2	Spring constant	k	12.75 kN/m
3	Flux density	B	0.7 T
4	Number of coil turns	N	50
5	Damping coefficient	c	0.75
6	Effective area of coil	A	$1.074 * 10^{-3} m^2$
7	Inverter inductor	$L_{z1} = L_{z2}$	1.2 mH
8	Inverter capacitor	$C_{z1} = C_{z2}$	15 μF
9	Nominal switching frequency	f	1250 Hz

A. Performance with Varying Frequency

The results of the 10-second simulation provide a comprehensive comparison of the performance of the actuator-based energy harvesting system when interfaced with both H-bridge and Z-source inverters under varying mechanical excitation frequencies. The force applied to the actuator was sinusoidal, with its frequency altered at different intervals—50 Hz between 1-2 seconds, 10 Hz between 2-7 seconds, and 75 Hz between 7-10 seconds. Figure 5 presents the force applied on the actuator and the corresponding EMF generated. Figure 6 presents the current generated by the actuator. The corresponding actuator-generated voltage and current reveals an emf with a peak of 4.7 V and a current of 100 mA. The voltage and current waveforms reflects the changes in the applied force, demonstrating the system's responsiveness to varying mechanical inputs. When examining the inverter output, both

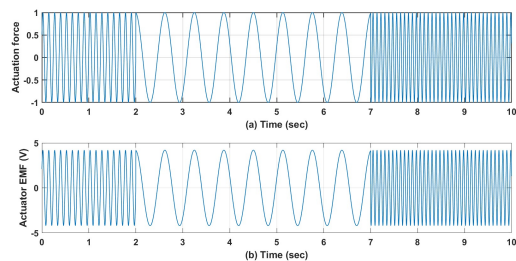


Fig. 5. (a) Force applied on the actuator (0-2 sec, 50 Hz; 2-7 sec, 10 Hz; 7-10 sec, 75 Hz) (b) EMF generated by actuator

the H-bridge and Z-source inverters produces voltage peaks of 10 V. However, their frequency response differed significantly, highlighting the distinct capabilities of each topology in adapting to the changing mechanical conditions. The H-bridge inverter's output voltage followed the applied force frequency during the first and last intervals (50 Hz between 1-2 seconds and 50 Hz between 7-10 seconds) but deviated during the middle interval, where it exhibited a frequency of 40 Hz instead of the expected 10 Hz. This deviation indicates the

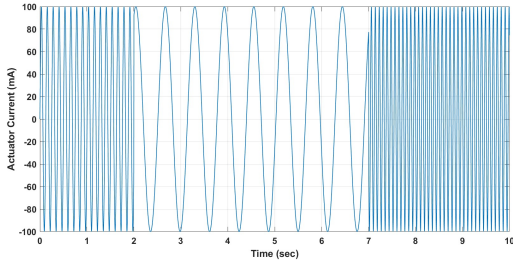


Fig. 6. Current developed by the actuator

H-bridge inverter's limitations in maintaining resonance with the mechanical system under varying excitation frequencies. Figure 7 presents the output voltage waveform of the H bridge inverter. In contrast, the Z-source inverter demonstrates

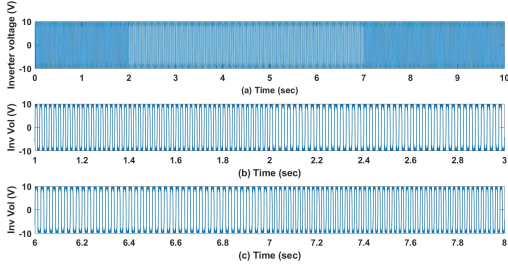


Fig. 7. (a) Voltage produced by H bridge inverter (b) Voltage waveform shown for 1-3 sec (c) Voltage waveform shown for 6-8 sec

superior performance in frequency tracking. It maintained a frequency of 50 Hz during the first interval (1-2 seconds), accurately followed the reduced frequency of 10 Hz during the second interval (2-7 seconds), and precisely matched the increased frequency of 75 Hz in the final interval (7-10 seconds). This ability to closely follow the mechanical system's resonant frequency throughout the simulation underscores the Z-source inverter's enhanced adaptability and efficiency in energy harvesting applications. Figure 8 presents the Z source inverter output. The results for the inverter currents further

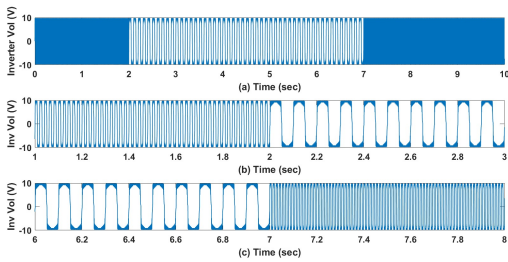


Fig. 8. (a) Voltage produced by Z source inverter (b) Voltage waveform shown for 1-3 sec (c) Voltage waveform shown for 6-8 sec

establish the fact as demonstrated with the voltage, with the Z-source inverter consistently outperforming the H-bridge inverter in tracking the mechanical system's frequency. The Z-source inverter's ability to dynamically adjust and maintain resonance with the varying mechanical frequencies resulted in more efficient energy conversion and better overall perfor-

mance. This demonstrates the Z-source inverter's superiority in applications where mechanical conditions are subject to change, making it a more robust choice for maximizing energy harvesting efficiency. Figure 8 and 9 presents the current waveform obtained with H bridge and Z source inverter topology respectively.

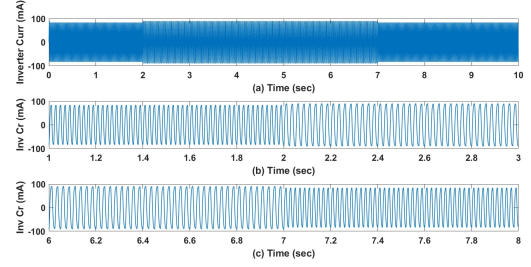


Fig. 9. (a) Current produced by H bridge inverter (b) Current waveform shown for 1-3 sec (c) Current waveform shown for 6-8 sec

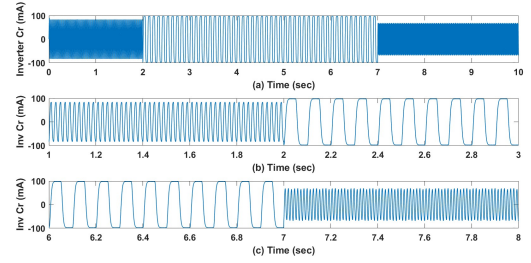


Fig. 10. (a) Current produced by Z source inverter (b) Current waveform shown for 1-3 sec (c) Current waveform shown for 6-8 sec

B. Performance with Varying Amplitude

In this additional simulation, the performance of the actuator-based energy harvesting system was evaluated under varying amplitude conditions, providing further insights into the comparative effectiveness of H-bridge and Z-source inverter topologies. The force applied to the actuator was sinusoidal with a constant frequency of 10 Hz, but with varying amplitudes: 0.75 between 1-2 seconds, 0.5 between 2-7 seconds, and 1 between 7-10 seconds. The resulting actuator-generated voltage and current were recorded, showing an emf with a peak of 5 V and a current of 100 mA. The voltage and current waveforms clearly exhibited changes corresponding to the fluctuations in the applied force, illustrating the system's responsiveness to varying mechanical input amplitudes. Figure 11 presents the actuator force, EMF generated and actuator current waveform. When analyzing the inverter output, both the H-bridge and Z-source inverters maintained a constant frequency of 10 Hz. However, their response to the varying amplitudes differed significantly. The H-bridge inverter produced voltage amplitudes of 6.5 V during the first interval (1-2 seconds), 5 V during the second interval (2-7 seconds), and 7 V during the final interval (7-10 seconds). These results indicate that while the H-bridge inverter was able to adjust to the changes in amplitude, it did so with some limitations,

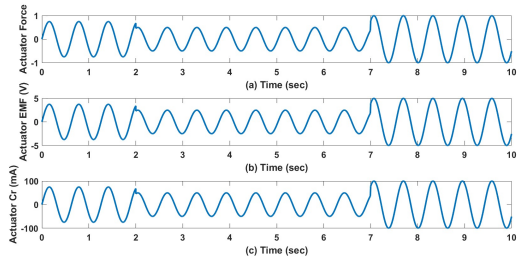


Fig. 11. (a) Force exerted on actuator (b) EMF produced by actuator (c) Current developed by the actuator

particularly in terms of the accuracy and extent of its response. Figure 12 presents the inverter output voltages for both the topologies.

On the other hand, the Z-source inverter demonstrated a more pronounced and accurate tracking of the varying amplitude. The voltage amplitude generated by the Z-source inverter was 7.5 V between 1-2 seconds, 5 V between 2-7 seconds, and 10 V between 7-10 seconds. This superior performance highlights the Z-source inverter's enhanced ability to adapt to changes in the mechanical system, effectively amplifying the voltage output in response to the increased force amplitude, especially during the final interval. The Z-source inverter's better amplitude tracking capability underscores its efficiency in maintaining optimal energy conversion under varying operating conditions. The inverter current results further confirmed

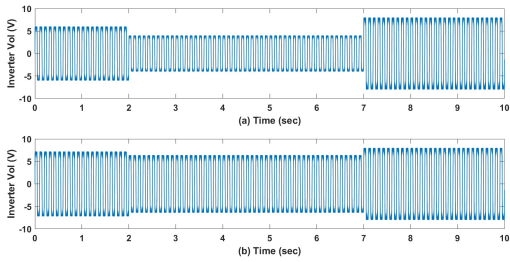


Fig. 12. (a) Inverter output voltage from Z source inverter (b) Voltage achieved from H bridge inverter

the Z-source inverter's superiority, as its output current more closely followed the variations in force amplitude, compared to the H-bridge inverter. Overall, the simulation results strongly suggest that the Z-source inverter topology is more adept at handling amplitude variations in the mechanical system, making it a more reliable and efficient choice for energy harvesting applications that involve fluctuating forces.

V. DISCUSSION

The simulation studies conducted for the actuator-based energy harvesting system provide critical insights into the performance and adaptability of different inverter topologies under varying mechanical conditions. The system's response was evaluated by applying sinusoidal forces with both varying frequency and amplitude, and the results were analyzed to compare the effectiveness of the conventional H-bridge inverter with the more advanced Z-source inverter topology.

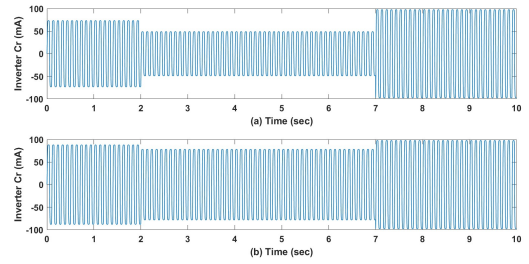


Fig. 13. (a) Inverter output current from Z source inverter (b) Current achieved from H bridge inverter

In the frequency variation study, the applied force was altered between 50 Hz, 10 Hz, and 75 Hz at different time intervals. The results showed that while both inverters could generate output voltages with the same peak of 10 V, their ability to track the frequency changes differed significantly. The H-bridge inverter exhibited a limited capacity to follow the changing frequencies, particularly in the mid-interval where it produced a frequency of 40 Hz instead of the expected 10 Hz. This discrepancy highlights the H-bridge inverter's limitations in maintaining resonance with the mechanical system, leading to suboptimal energy harvesting efficiency. Conversely, the Z-source inverter demonstrated a robust frequency tracking ability, accurately matching the mechanical system's frequency throughout the entire simulation period. This consistent performance underscores the Z-source inverter's superior adaptability, making it more effective in harnessing energy under varying frequency conditions. Similarly, the amplitude variation study further emphasized the advantages of the Z-source inverter. Here, the force was applied with a constant frequency of 10 Hz but with varying amplitudes of 0.75, 0.5, and 1. The H-bridge inverter, while capable of adjusting to these amplitude changes, did so with less precision, particularly in its voltage output, which ranged from 5 V to 7 V depending on the interval. In contrast, the Z-source inverter not only matched the frequency but also demonstrated a more accurate and efficient response to the amplitude variations, with its output voltage ranging from 5 V to 10 V. This indicates a better tracking capability and an enhanced ability to maximize energy extraction from the fluctuating force.

The inverter current analysis across both studies corroborated these findings, with the Z-source inverter consistently outperforming the H-bridge inverter in both frequency and amplitude tracking. The results clearly show that the Z-source inverter's ability to dynamically adjust its operation, particularly through shoot-through control, enables it to maintain resonance with the mechanical system under varying conditions, leading to higher power density and more efficient energy conversion.

Overall, these simulation studies confirm that while the H-bridge inverter can function effectively under stable conditions, it falls short when dealing with dynamic mechanical inputs. The Z-source inverter, with its superior adaptability, is better suited for actuator-based energy harvesting systems, particularly in applications where the mechanical input is subject to frequent changes in frequency and amplitude. The

findings of this study provide a compelling case for the use of Z-source inverter topology in advanced energy harvesting systems, offering improved efficiency and performance in real-world scenarios.

VI. CONCLUSIONS

This work presents a novel Z source inverter based energy harvesting system. The performance of an actuator-based energy harvesting system under varying mechanical conditions has been investigated, focusing on the comparison between conventional H-bridge and proposed Z-source inverter topologies. The methodology involves simulating the system's response to sinusoidal forces with varying frequencies and amplitudes over a 10-second period. An investigation into the system's ability to maintain resonance and optimize energy conversion under these dynamic conditions has been conducted. The findings revealed that while the H-bridge inverter struggled to accurately track changes in frequency and amplitude, the Z-source inverter demonstrated superior adaptability, maintaining resonance and efficiently harnessing energy across the full range of operating conditions. This proposed energy harvesting system architecture establish the Z-source inverter's potential for enhancing the efficiency and performance of energy harvesting systems, particularly in applications where mechanical inputs are subject to frequent fluctuations.

REFERENCES

- [1] N. Herisanu, B. Marinca, and V. Marinca, "Dynamic analysis of a uniform microbeam resting on a nonlinear foundation considering its curvature subjected to a mechanical impact and electromagnetic actuation," *Micromachines*, vol. 15, no. 8, 2024. [Online]. Available: <https://www.mdpi.com/2072-666X/15/8/969>
- [2] S. Chauvière, L. Belguerras, T. Lubin, S. Mezani, S. Leclerc, and L. Guendouz, "Magnetic resonance imaging-compatible electromagnetic actuator: Design and tests," *Energies*, vol. 17, no. 13, 2024. [Online]. Available: <https://www.mdpi.com/1996-1073/17/13/3254>
- [3] D. K. Han and J. H. Chang, "Design of electromagnetic linear actuator using the equivalent magnetic circuit method," *IEEE Transactions on Magnetics*, vol. 52, no. 3, pp. 1–4, 2016.
- [4] M. Markovic, M. Jufer, and Y. Perriard, "Analytical force determination in an electromagnetic actuator," *IEEE Transactions on Magnetics*, vol. 44, no. 9, pp. 2181–2185, 2008.
- [5] P. Jin, H. Lin, S. Fang, Y. Yuan, Y. Guo, and Z. Jia, "3-d analytical linear force and rotary torque analysis of linear and rotary permanent magnet actuator," *IEEE Transactions on Magnetics*, vol. 49, no. 7, pp. 3989–3992, 2013.
- [6] A. A. Rendon-Hernandez, J. Desforges, and S. Follic, "Testing, modeling, and simulation of a miniature electromagnetic harvesting power generator for self-powered, connected wireless switch," in *2022 21st International Conference on Micro and Nanotechnology for Power Generation and Energy Conversion Applications (PowerMEMS)*, 2022, pp. 166–169.
- [7] Y. Li, C. Zhou, X. Wang, J. Wang, D. Qiao, and K. Tao, "A vibration energy harvester with targeted frequency-tuning capability," *IEEE Transactions on Instrumentation and Measurement*, vol. 71, pp. 1–10, 2022.
- [8] R. Gherca and R. Olaru, "Power analysis for an electromagnetic generator with magnets destined to vibration energy harvesting," in *2012 International Conference and Exposition on Electrical and Power Engineering*, 2012, pp. 485–490.
- [9] J. A. Bowden, S. G. Burrow, A. Cammarano, L. R. Clare, and P. D. Mitcheson, "Switched-mode load impedance synthesis to parametrically tune electromagnetic vibration energy harvesters," *IEEE/ASME Transactions on Mechatronics*, vol. 20, no. 2, pp. 603–610, 2015.
- [10] B.-C. Lee and G.-S. Chung, "A novel frequency tuning design for vibration-driven electromagnetic energy harvester," in *2015 IEEE SENSORS*, 2015, pp. 1–4.
- [11] P. D. Mitcheson, T. T. Toh, K. H. Wong, S. G. Burrow, and A. S. Holmes, "Tuning the resonant frequency and damping of an electromagnetic energy harvester using power electronics," *IEEE Transactions on Circuits and Systems II: Express Briefs*, vol. 58, no. 12, pp. 792–796, 2011.
- [12] R. Adhikari and N. Jackson, "Passive frequency tuning of piezoelectric energy harvester using embedded masses," in *2021 IEEE 20th International Conference on Micro and Nanotechnology for Power Generation and Energy Conversion Applications (PowerMEMS)*, 2021, pp. 176–179.
- [13] S. Su, B. D. Truong, S. Aunet, and C. P. Le, "A reliable and wide-range tuning technique for low-frequency mems energy harvesters," in *2021 IEEE 20th International Conference on Micro and Nanotechnology for Power Generation and Energy Conversion Applications (PowerMEMS)*, 2021, pp. 76–79.
- [14] A. Pechhacker, D. Wertjan, E. Csencsics, and G. Schitter, "Integrated electromagnetic actuator with adaptable zero power gravity compensation," *IEEE Transactions on Industrial Electronics*, vol. 71, no. 5, pp. 5055–5062, 2024.
- [15] Y.-D. Chen and C.-H. Liu, "Rotationally tunable frequency selective surfaces for large areas via linkage mechanisms," in *2017 IEEE International Symposium on Antennas and Propagation USNC/URSI National Radio Science Meeting*, 2017, pp. 265–266.
- [16] L. Dhakar, H. Liu, F. Tay, and C. Lee, "A new energy harvester design for high power output at low frequencies," *Sensors and Actuators A: Physical*, vol. 199, pp. 344–352, 2013. [Online]. Available: <https://www.sciencedirect.com/science/article/pii/S092442471300294X>
- [17] M. Pamujula, A. Ohja, R. Kulkarni, and P. Swarnkar, "Cascaded 'h' bridge based multilevel inverter topologies: A review," in *2020 International Conference for Emerging Technology (INCET)*, 2020, pp. 1–7.
- [18] F. Khoucha, M. S. Lagoun, A. Kheloui, and M. E. H. Benbouzid, "A comparison of symmetrical and asymmetrical three-phase h-bridge multilevel inverter for dte induction motor drives," *IEEE Transactions on Energy Conversion*, vol. 26, no. 1, pp. 64–72, 2011.
- [19] M. Sadoughi, A. Pourdardashnia, M. Farhadi-Kangarlu, and S. Galvani, "Pso-optimized she-pwm technique in a cascaded h-bridge multilevel inverter for variable output voltage applications," *IEEE Transactions on Power Electronics*, vol. 37, no. 7, pp. 8065–8075, 2022.
- [20] M. M. Hasan, A. Abu-Siada, S. M. Islam, and M. S. A. Dahidah, "A new cascaded multilevel inverter topology with galvanic isolation," *IEEE Transactions on Industry Applications*, vol. 54, no. 4, pp. 3463–3472, 2018.
- [21] N. Karania, M. A. AlalI, S. Di Gennaro, and J.-P. Barbot, "Developed ac/dc/ac converter structure based on shunt active filter and advanced modulation approach for asymmetrical cascade h-bridge multilevel inverters," *IEEE Open Journal of the Industrial Electronics Society*, vol. 4, pp. 583–602, 2023.
- [22] T. Debnath, K. Gopakumar, L. Umanand, K. RajaShekara, and D. Zielinski, "A generalized multilevel inverter with extended linear modulation range and instantaneously balanced dc-link series capacitors for an induction motor drive," *IEEE Journal of Emerging and Selected Topics in Power Electronics*, vol. 11, no. 2, pp. 2104–2113, 2023.